中國機械工程學刊第三十六卷第一期第 67~73 頁(民國一百零四年)
Journal of the Chinese Society of Mechanical Engineers, Vol.36, No.1, pp 67~73 (2015)

Process Parameters Analyses on Stainless Steel Circle Cup by Micro Drawing Process

Tsung-Chia Chen* and Xaio-Yuan Wang**

Keywords: finite element, micro circle cup, micro drawing, die angle.

ABSTRACT

This study used a micro drawing to determine the effects of die angle (α=-15°~15°) on the formability of micro circle cups. A program for finite element analysis of incremental elastic-plasticity deformation is developed by combining the flow rule of Prandtl-Reuss with finite element deformation theory and the stress-strain relation of correction materials. The program is then used to simulate the circle cup micro drawing process. The program uses general r_{min} algorithm to solve problems of elastic-plasticity status and die contact. Simulations performed using the finite element analysis program acquire the relations among deformation, punch load, stroke, thickness distribution, stress, and strain distribution during the circle cup micro drawing process, which indicate the changes in the forming process. The simulation was consistent with experimental results, *i.e.*, easily-cracked areas in the micro circle cup forming process appear on the punch fillet.

INTRODUCTION

Metal sheet stamping is one of the most common forming processes. Although the process is simple, many technological problems can occur during stamping processes, including estimated springback (after sheet forming) for the die design; process control; accuracy of workpiece shape; cracks resulting from stretching of the workpiece surface; and estimation of punch load and selection of proper drawing equipment in the drawing process (Lin et al., 2010; Zhang et al., 2010). The emergence of modern micro processing methods and the miniaturizatin of components have resulted in differences between micro processing and macro processing. Since conventional macro processing theory is not directly applicable in micro forming processes, micro-plastic forming theory and technology should be re-inspected (Qin, 2006; Vollertsen et al., 2004).

By placing a sheet in the circle cup micro drawing die, a punch can be used to stamp the sheet into the mold and form the micro circle cup. After completing the micro drawing process, the formed workpiece is removed from the die. Removing the load causes the workpiece to spring back to its final size. The remaining stress is balanced, and the unloading and springback process determine the final shape of the product. The elastic-plasticity finite element analysis (FEA) program is based on the updated Lagrangian formulation (ULF), which effectively simulates the micro drawing process, and on selective reduced integration method (Hughes, 1980), which has proved effective for anisotropic and non-linear metal forming processes. Modified Coulomb Friction rules are also used to solve discontinuous viscosity and glide between contact surfaces.

The FEA program can acquire workpiece shape, thickness distribution, stress and strain distribution, crack, and drawing forming limits. Therefore, numerical simulations must be performed in advance to predict cracks and the conformance to the required geometric shape. Such a method can achieve lower costs compared to conventional trial and error methods.

BASIC THEORY

Basic Hypothesis

The blank considered in this study is made several assumptions in the elasto-plastic deformation.

1. The material is assumed homogeneous.
2. The material is assumed planar anisotropic.
3. The material satisfies Hooke's Law in the elasticity area.
4. Dies are regarded as the rigid body.
5. The effect of residual stress is not considered in the material forming.
6. The effect of temperature is not considered in the

Paper Received June, 2014. Revised September, 2014, Accepted October, 2014, Author for Correspondence: Tsung-Chia Chen.

* *Professor, Department of Mechanical Engineering, National Chin-Yi University of Technology, Taichung, Taiwan 41170, ROC.*

** *Graduated Student, Department of Mechanical Engineering, National, Chin-Yi University of Technology, Taichung, Taiwan 41170, ROC.*

material forming.

Principle Variation

The updated Lagrangian formulation (ULF) is modified according to the virtual velocity (McMeeking et al., 1975).

$$\int_V \{(\sigma_{ij}^J - 2\sigma_{ik}D_{ik})\delta D_{ij} + \sigma_{jk}L_{ik}\delta L_{ij}\}dV = \int_{S_t} \dot{f}_i \delta v_i dS \qquad (1)$$

where σ_{ij}^J is the Jaumann rate of the Cauchy stress tensor, σ_{ij} is the Cauchy stress tensor, L_{ik} is the velocity gradient ($L_{ik} = \partial v / \partial x$), D_{ik} is the strain rate, V and S_t are the material volume and the external surface area, respectively, and δv_i and $\dot{f}_i$ are the virtual velocity and the tensor of surface tension per unit area change, respectively. Additionally, $\det(\partial v / \partial x \cong 1)$ that $\tau^J = \sigma^J$, where τ^J is the Kirchhoff stress derived from Jaumann. The program can be used to define a small strain, linear flexibility, and the plasticity of large deformation and work hardening (Cao and Teodosiu, 1989).

$$\sigma_{ij}^J = C_{ijkl}^{ep} D_{kl} = C_{ijkl}^{ep} L_{kl} \qquad (2)$$

Where C_{ijkl}^{ep} is the elastic-plasticity tensor. According to the virtual velocity principle, Eq. (2) can be substituted for Eq. (1).

$$\int_V \bar{C}_{ijkl} L_{kl} \delta L_{ij} dV = \int_{S_t} \dot{f}_i \delta v_i dS \qquad (3)$$

where, $\bar{C}_{ijkl} = C_{ijkl}^{ep} + \Omega_{ijkl}$;

$$\Omega_{ijkl} = \frac{1}{2}\left(\sigma_{jl}\delta_{ik} - \sigma_{ik}\delta_{jl} - \sigma_{il}\delta_{jk} - \sigma_{jk}\delta_{il}\right).$$

Stiffness Equation

The above problems can be solved by standard methods. Equation (3) is complete from time $t \to t + \Delta t$, where Δt is the micro time increment. When using finite element method for discretization, an algebraic equation can be used instead of Eq. (3).

$$K\Delta u = \Delta F + \Delta C \qquad (4)$$

where K is the stiffness matrix of elastic-plasticity, Δu is the incremental node displacement, and ΔF and ΔC are the changes on the right side of Eq. (3). Stiffness matrix K, which is a constant, is used to describe time t and the time increment Δt. The $r_{\min}$ rule described above (Yamada et al., 1968) is used to restrict the increment.

Selective Reduced Integration Method (SRI)

Since volume is uncompressible (constant) in a plastic forming process, FEA of the sheet would be overly restricted if all integration rules were satisfied. In this case, shear strains γ_{xz} and γ_{yz} would be set to zero during sheet deformation (Hinton et al., 1984). The FEA program developed by Hughes (1980) used SRI to solve volume uncompressible problems (Hughes, 1987).

Weighting Factor $r_{\min}$ for the Increment of Each Loading Step

During each increment, the material is referred to its configuration at the beginning of the increment (updated Lagrangian scheme). The contact and separation conditions of nodes and the state of elements must remain invariable during the increment. In order to satisfy this requirement and to assure the accuracy of this explicit integration scheme (static explicit formulation), the weighting factor $r_{\min}$ proposed by Yamada et al. (1968) is used to treat the elastic-plastic and contact-separation problems to choose the size of the increment to keep linear relation. The size of each loading step is determined by the smallest value of the following five r-values, $r_{\min} = \text{MIN}(r_1, r_2, r_3, r_4, r_5)$:

r_1: To ascertain the equivalent stress of elastic element just reaches the current yield surface

r_2: To limit the largest equivalent strain increment to linear relation

r_3: To limit the rotation increment to linear relation

r_4: For making a free node just contact with the tools

r_5: For making a contact node just depart from the tool surface

The above is proved valid in the first order theory. More detailed information of weighting factor $r_{\min}$ can be found in (Leu, 1996).

Correction Factors in Micro Material Model

The micro drawing process requires a new material model for a metal sheet since the materials presently used in micro-forming make a macro material model unsuitable for micro-forming process. Therefore, sheet thickness is used as the correction factor in the macro material model in this study, which applies the Swift material model as shown below.

$$\bar{\sigma} = K(\varepsilon_0 + \bar{\varepsilon}_p)^n \qquad (5)$$

The size effect is important when the sheet thickness is less than 1.0mm but not when the sheet thickness is larger than 1.0mm. The sheet thickness used in this study is 0.05mm that the sheet thickness is used for modifying the material model (5).

$$\bar{\sigma}(t, \bar{\varepsilon}) = aKe^{bt}(\varepsilon_0 + \bar{\varepsilon}_p)^{n(ce^{dt}-1)} \qquad (6)$$

where a, b, c, d are the correction values and t is the

sheet thickness. The correction values reported in Liu (2006) are substituted into the equation.

$$\bar{\sigma}(t,\bar{\varepsilon}) = 0.73667Ke^{0.3152t}(\varepsilon_0 + \bar{\varepsilon}_p)^{n(1.0106e^{-0.01029t}-1)} \quad (7)$$

For an FEA of the modified material parameters, the experimental results are further compared to determine whether the modified material parameters provide a better simulation of the micro-forming process.

EXPERIMENTAL SETUP AND NUMERICAL ANALYSIS

This study used quadrilateral four-node shells to deduce the stiffness matrix. The model is axial symmetric, and a 1/4 model is used to save time. The sheet and the die are drawn with CAD for mesh segmentation, which is transferred into data files for numerical analyses in the incremental elastic-plasticity deformation FEA program. The simulation results are entered in CAD for further interpretation. The CAD drawings show the deformation and the stress-strain distribution, which can be used for the reference during the die design and micro drawing processes.

Die Setting

Figure 1 shows the SUS304 stainless steel sheets used in this study, which had diameters of 2.5mm, 3.0mm, and 4.0mm. The blank had a thickness of 0.05mm. Table 1 shows the material parameters after correction for scale factors.

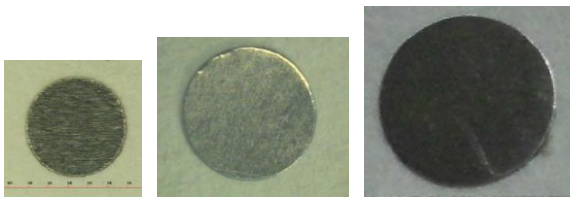

D_0=2.5mm D_0=3.0mm D_0=4.0mm

Fig. 1. The SUS304 stainless steel sheet (t=0.05mm) used in the experiment.

Table 1. Material parameters of the blank.

Material	E(GPa)	σ_y (MPa)	K(MPa)	n	ε_0
SUS 304	198	306	1361	0.582	0.077

The true stress-strain curve is approximated by $\bar{\sigma} = K(\varepsilon_0 + \bar{\varepsilon}_p)^n$; υ=0.3; E: Young modulus; and σ_y: yield stress.

In the simulated stainless steel circle cup angle micro drawing, quadrilateral elements are applied to the die mesh segmentation. Figure 2 shows the design of stainless steel circle cup angle micro drawing module, Figure 3 shows the solid parts of the die, and Table 2 presents the die size.

In the micro drawing process, the effects of sheet radius (D_0) and die angle (α in Table 3) on the stainless steel circle cup angle micro drawing process are discussed to analyze the relations among deformation, punch load, stroke, thickness distribution, and stress-strain distribution during the forming process.

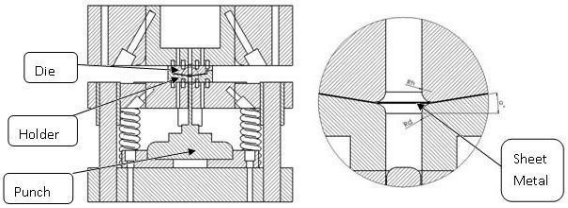

Fig. 2. Stainless steel circle cup angle micro drawing module diagram.

Fig. 3. Solid parts of the die.

Table 2. Die sizes.

Dies	Dimension
Diameter of punch (D_P)	2.0 mm
Fillet radius of die (R_D)	0.6 mm
Fillet radius of holder (R_H)	0.6 mm
Fillet radius of punch (R_P)	0.6 mm
Die angle (α)	0°
Die gap	0.055 mm

Table 3. Die angle.

α (degree)	-15	-9	0	9	15

Boundary Condition

During the stainless steel circle cup angle micro drawing process, the blank comes in contact with the punch, mold, and blank holder. Therefore, all nodes of the blank must be defined whether or not they are in contact with the die. The nodes can be classified

contact nodes and free nodes. The free nodes are indicated by global coordinates (X, Y, Z), and the contact nodes are indicated by local coordinates (ξ, η, ζ). Single arrow indicates the displacement is constrained, and double arrows indicate the rotation is constrained. Figure 4 shows the boundary conditions when the blank is combined with the die system.

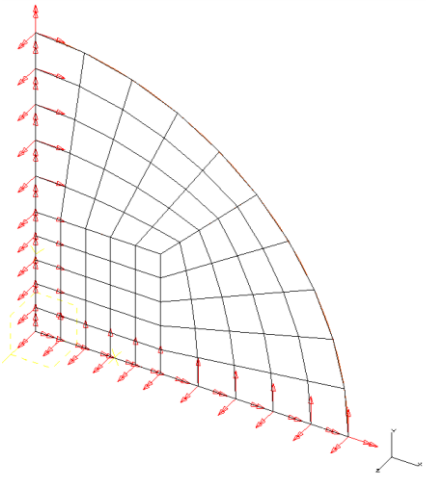

Fig. 4. Sheet meshing and boundary settings.

The contact surface between the blank and the die is affected by glide and viscosity. The calculation is complicated when friction is considered. Saran & Wagoner (1991) and Oden & Pries (1983) have suggested modifying the Coulomb Friction rules to include friction of glide and viscosity. Such rules effectively solve the viscosity-glide friction problem of discontinuous glide direction. The simulation of the stainless steel circle cup angle micro drawing process describes the friction condition by assuming the coefficient of friction μ= 0.05.

Process of Elastic-Plasticity

As deformation increases, the elasticity and plasticity of the blank should be pre-judged at each increment so that the element remains constant at each increment. The r_{min} rule is also used to judge the elastic-plasticity status.

Process of Unloading

Sicne springback is a key factor in the circle cup angle micro drawing process, sheet forming after unloading should be considered. When the die is completely removed, the springback is calculated, and the boundary condition of the new force is designated on all contacting nodes and set as $\Delta f = -f$.

RESULT AND DISCUSSION

This study analyzed the effects of die angles on the circle cup micro drawing process. The changes in the forming process are observed according to the relations among deformation data, punch load and stroke, thickness distribution, and stress-strain distribution. The experimental results for a die angle of 0° are first compared with the simulation results to verify the reliability of the analysis program.

Figure 5 shows the five-stage deformation at the die angle 0°. During micro drawing, the sheet gradually deforms until it reaches unloading status. Throughout the entire micro drawing process, the contact, separation, and overall friction are calculated by using the r_{min} rule. Figure 6 compares the relations between the punch load and the punch stroke among the three sheet sizes (D_0=2.5, 3.0, 4.0). The punch load at the initial forming increases as the stroke increases. However, the difference between the punch load and stroke increases when the stroke reaches 0.1mm. After remaining at a certain load, the curve rises rapidly as the contact surfaces of the die and blank enlarge.

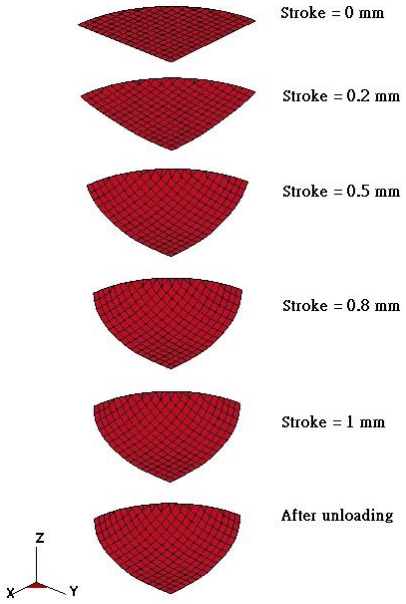

Fig. 5. Deformation of circle cup micro drawing process.

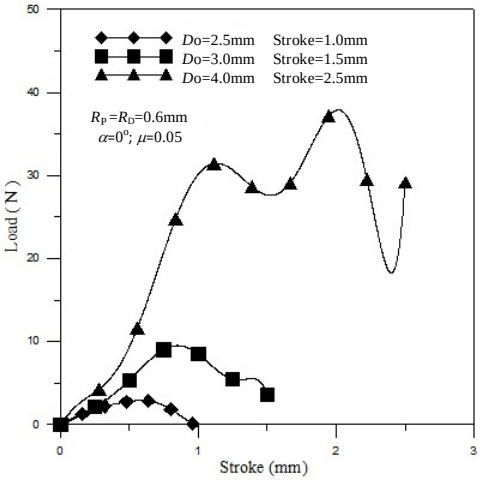

Fig. 6. Relation between punch load and stroke.

Figure 7 compares the distribution of stress in different sheet sizes. Stress is highest at the cup edge because of the material flowing violently in the area. Comparisons of the three drawings show that stress is highest at the circle cup with D_0=4.0mm (approximately 930MPa) and lowest at the circle cup with D_0=2.5mm (approximately 416 MPa). The difference is 514MPa, and the circle cup with D_0=4.0mm approaches the drawing limit at which cracks are likely to result from excessive stress in the micro drawing process.

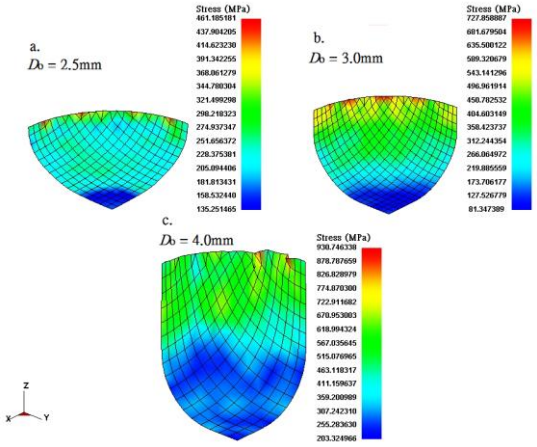

Fig. 7. Stress distribution in different sheet sizes.

Figure 8 shows the strain distribution of various sheet sizes. The maximal strain also appears on the cup edge; additionally, strain is highest in the circle cup with D_0=4.0mm (approximately 0.746) and lowest in the circle cup with D_0=2.5mm (approximately 0.103).

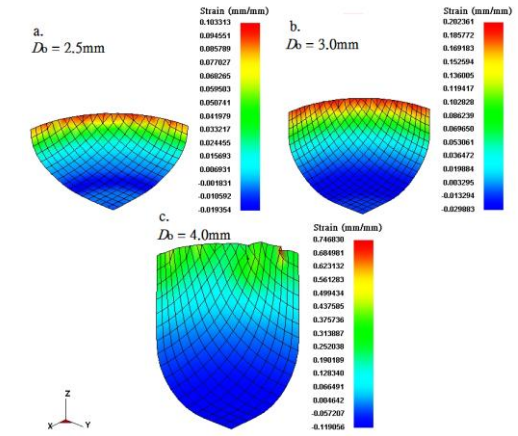

Fig. 8. Strain distribution in different sheet sizes.

Figure 9 compares the thickness distribution of different sheet sizes. The thinnest part appears at the punch fillet. Comparison of the three sheet sizes shows that the thinnest part is on the circle cup with D_0=4.0mm, about 0.044mm, and the larger sheet radius could easily result in ripples. The thickness of the blank is 0.05mm. An important engineering consideration is that, in all three blanks sizes, a crack thickness of 0.025mm would not cause cracks on the micro circle cup.

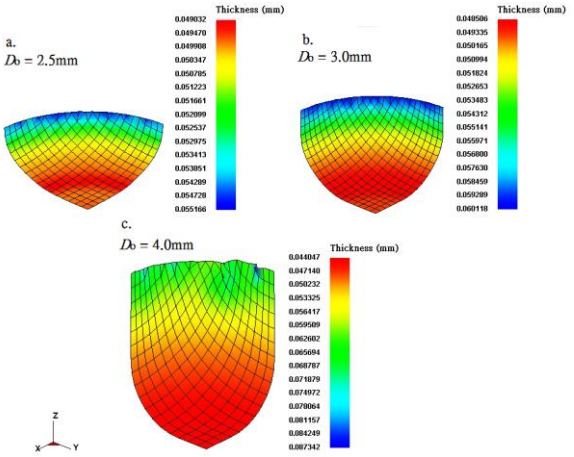

Fig. 9. Thickness distribution in different sheet sizes.

Figure 10 compares shapes and heights between the experimental and simulated micro circle cups. The results reveal few differences in the shapes and heights, which confirms the reliability of the analysis program.

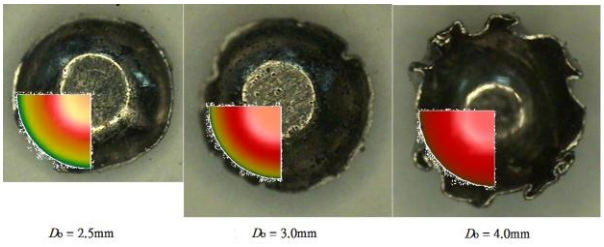

(a)

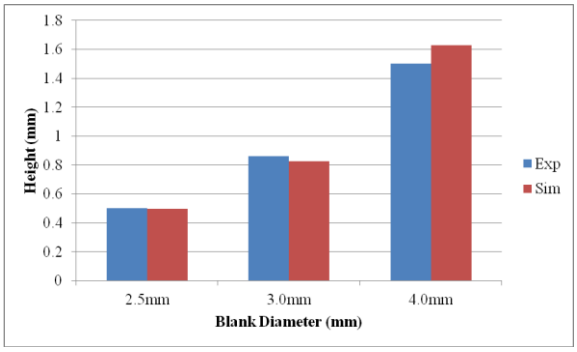

(b)

Fig. 10. Comparison of experimental and simulated micro circle cup (a) shape and (b) height.

Figure 11 shows the effects of die angles (α=-15°~15°) on punch load and stroke. The punch load increases as punch stroke increases. When die angle=15°, the blank can easily flow because the load is reduced; the maximal load approaches 9.44N. When the load appears on the peak, the maximal load appears on the die angle=-15°, and the load approaches 9.67N. When the die angle tilts downwards (positive), the larger angle decreases the load as it easily flows at larger angles.

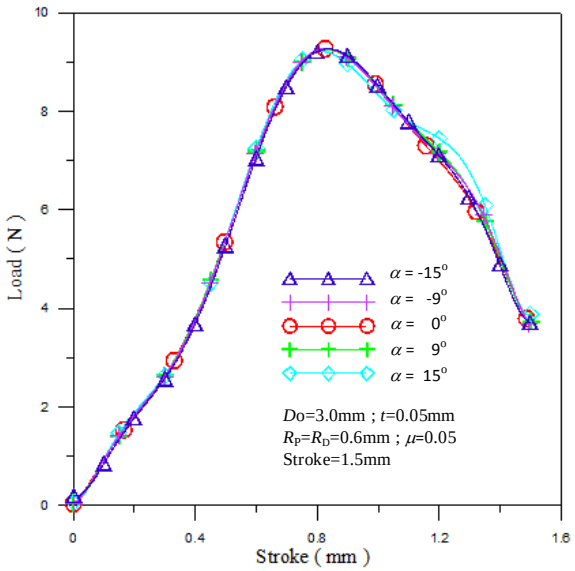

Fig. 11. Effects of die angle on punch load and stroke.

Figure 12 shows the effects of a modified coefficient of friction on punch load and punch stroke: the punch load increases as the coefficient of friction increases.

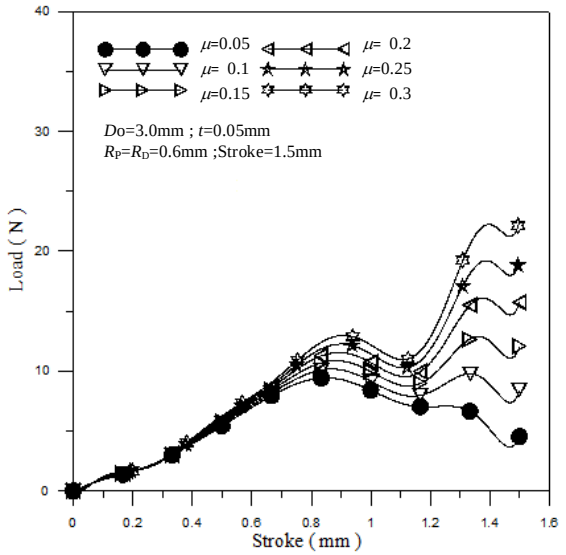

Fig. 12. Effects of coefficient of friction on punch load and stroke.

Figure 13 shows the effects of modified die fillet radius on punch load and stroke: the punch load increases as punch stroke increases. As the die fillet radius increases, the punch load decreases. The maximal load approaches 17N when R_D=R_P=0.2mm; the minimum load approximates 9N when R_D=R_P =0.6mm.

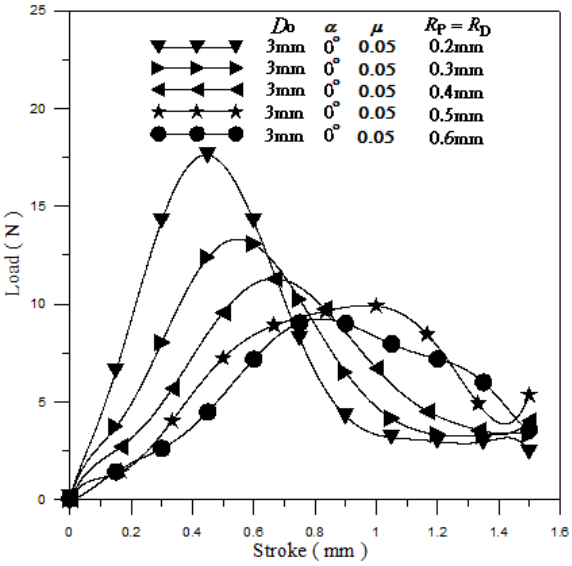

Fig. 13. Effects of die fillet radius on punch load and stroke.

CONCLUSIONS

This study performed an FEA of incremental elastic-plasticity deformation and used SRI method to develop a program for simulating metal sheet micro drawing. Increment is used for the non-linear management, and the r_{min} rule is used to restrict the increment gap so that the calculation process becomes linear. The conclusions are summarized as follows.

1. The FEA provides precise and complete analysis of deformation in the stainless steel circle cup angle micro drawing process, meaning to successfully draw the entire deformation process.
2. The punch load increases as punch stroke increases. As the angle increases, the load decreases. When the die angle tilts downwards (positive), the larger angle causes an easier flow.
3. Comparisons showed that a high coefficient of friction results in a high punch load.
4. In the circle cup angle micro drawing process, the thinnest part is the punch fillet. Comparisons of the three sheet sizes showed that the thinnest part was the circle cup with D_0=4.0mm. A larger sheet radius would tend to cause ripples.

ACKNOWLEDGMENT

This paper was supported by the National Science Council, Taiwan, Republic of China, through Grant NSC 102-2221-E-167-004. We are grateful to the National Center for High-performance Computing for computer time and facilities.

REFERENCES

Cao, H.L., and Teodosiu, C., "Finite element calculation of springback effects and residual stress after 2D deep drawing," *Conference proceedings: Computational Plasticity - fundamentals and applications*, Barcelona, Spain (1989).

Hinton, E., and Owen, D.R., "*Finite Element Software for Plates and Shell*," Swansea, UK: Pineridge (1984).

Hughes, T.J.R., "Generalization of selective integration procedures to anisotropic and nonlinear media," *International Journal for Numerical Methods in Engineering*, Vol.15, No.9, pp.1413-1418 (1980).

Hughes, T.J.R., "*The Finite Element Method*," Englewood Cliffs, NJ: Prentice-Hall (1987).

Leu, D.K., "Finite-element simulation of hole-flanging process of circular sheets of anisotropic materials," *International Journal of Mechanical Sciences*, Vol.38, No.8-9, pp.917-933 (1996).

Lin, J.F., Li, F., Yuan, S.J., and Han, J.C., "Research on Hydroforming Tubular Parts with Dissymmetrical Structure," *Journal of the Chinese Society of Mechanical Engineers*, Vol.31, No.4, pp.335-339 (2010).

McMeeking, R.M., and Rice, J.R., "Finite-element formulations for problems of large elastic-plastic deformation," *International Journal of Solids and Structures*, Vol.11, pp.601-616 (1975).

Oden, J.T., and Pries, E.B., "Nonlocal and nonlinear friction laws and variational principles for contact problems in elasticity," *Transactions of ASME, Journal of Applied Mechanics*, Vol.50, No.1, pp.67-76 (1983).

Liu, F., "Study on the Key Technology of Micro-forming Process," *Postdoctoral Thesis*, Shanghai Jiao Tong University, Shanghai, China (2006).

Qin, Y., "Micro-forming and miniature manufacturing systems - development needs and perspectives," *Journal of Materials Processing Technology*, Vol.177, pp.8-18 (2006).

Saran, M.J., and Wagoner, R.H., "Consistent implicit formulation for nonlinear finite element modeling with contact and friction. Part I. Theory," *Transactions of ASME, Journal of Applied Mechanics*, Vol.58, No.2, pp.499-506 (1991).

Vollertsen, F., Hu, Z., Schulze Niehoff, H., and Theiler, C., "State of the art in micro forming and investigations into micro deep drawing," *Journal of Materials Processing Technology*, Vol.151, pp.70-79 (2004).

Yamada, Y., Yoshimura, N., and Sakurai, T., "Plastic stress-strain matrix and its application for the solution of elastic-plastic problems by the finite-element method," *International Journal of Mechanical Sciences*, Vol.10, pp.343-354 (1968).

Zhang, Z.C., Manabe, K., Zhu, F.X., Mirzai, M.A., and Li, T.H., "Evaluation of Hydroformability of TRIP Steel Tube by Flaring Test," *Journal of the Chinese Society of Mechanical Engineers*, Vol.31, No.5, pp.375-382 (2010).

不鏽鋼圓杯微引伸製程參數之分析

陳聰嘉　王筱媛
國立勤益科技大學 機械工程系

摘 要

本研究之目的在於探討不同模具角度(α=-15°~15°)對於製作微形圓杯之影響，並進行微引伸實驗來分析模具角度對微形圓杯成形性之影響。本文以 Prandtl-Reuss 之塑流法則，結合有限元素變形理論與修正材料的應力-應變關係式，建立一增量型彈塑性變形有限元素分析程式，來模擬圓杯微引伸製程，此分析程式是採用廣義之 r_{min} 演算法處理彈塑性狀態與模具接觸面之接觸問題。藉由有限元素分析程式的模擬，可獲得圓杯微引伸製程的全部變形履歷、衝頭負荷與衝程之關係、厚度分佈以及應力與應變的分佈圖，藉以觀察成形過程之變化。將模擬與實驗結果做比較，獲得相當一致性之趨勢；亦顯示微形圓杯成形製程，容易產生破裂之區域，均發生在杯緣處。